

## METHOD

# Coupled in vitro synthesis and splicing of RNA polymerase II transcripts

SAGARMOY GHOSH<sup>1</sup> and MARIANO A. GARCIA-BLANCO<sup>1,2</sup>

<sup>1</sup>Department of Genetics, Duke University Medical Center, Durham, North Carolina 27710, USA

<sup>2</sup>Departments of Microbiology and Medicine, Duke University Medical Center, Durham, North Carolina 27710, USA

## ABSTRACT

Compelling in vivo studies suggest a tight functional linkage between RNA polymerase II transcription and pre-messenger RNA splicing. At present, the specific interactions involved in this coupling are poorly understood and deserve investigation. To this end, we developed an in vitro system that permits study of coupled transcription and splicing. Transcripts generated by RNA polymerase II were accurately and efficiently spliced under reaction conditions that permitted both transcription and splicing to occur simultaneously. The splicing of RNA-polymerase-II-driven transcripts was accelerated relative to that of the same transcripts driven by T7 RNA polymerase. Moreover, the product of exon ligation was found associated with the DNA template in reactions driven by RNA polymerase II. These two findings indicate that transcription and splicing were coupled in the in vitro system driven by RNA polymerase II, and suggest that this system will be useful for the biochemical study of this coupling.

**Keywords:** cotranscriptional splicing; rate of splicing; RNA polymerase II; T7 RNA polymerase; transcription

## INTRODUCTION

In vivo studies strongly suggest that nascent transcripts synthesized by RNA polymerase II (RNAP II) are assembled into splicing complexes and undergo splicing. Miller chromatin spreads reveal assembly of RNP particles, presumed to be spliceosomes, and shortening of nascent transcripts, interpreted as intron removal, in genes of *Drosophila melanogaster* embryos (Beyer & Osheim, 1988). Further evidence for cotranscriptional splicing was noted in RNAs originating from the Balbani ring 1 in the dipteran *Chironomus tentans* in which the intron was shown to be removed from the transcript within the first 2.5 min after the start of the transcription (Bauren & Wieslander, 1994). Recruitment of splicing factors to sites of active viral transcription in HeLa cells infected with adenovirus 2 suggests that splicing factors can be mobilized from sites of storage to transcription sites (Jimenez-Garcia & Spector, 1993). Moreover, in mammalian cells, introns are detected only in very close proximity to the gene of origin, implying that intron removal occurs at, or very near,

sites of transcription (Zhang et al., 1994). Functional studies also reveal links between transcription and splicing. A role of promoter sequences in alternative splice site choice has been reported for the fibronectin EDI exon; the response to SR proteins depends on the promoter sequences driving transcription (Cramer et al., 1997, 1999). This suggests the assembly of an exon-specific polymerase complex. In another study, commitment to a specific splicing outcome was determined cotranscriptionally (Roberts et al., 1998), again implying linkage between splicing regulation and transcription.

Biochemical evidence of cotranscriptional mRNA processing has focused on the role of the C-terminal domain (CTD) of the largest subunit of RNAP II, a unique feature of this polymerase. In human cells, the CTD contains 52 repeats of the YSPTSPS motif (Greenleaf, 1993; Corden & Patturajan, 1997; Neugebauer & Roth, 1997; Bentley, 1999). Several findings suggest a role for the CTD as a platform for coupling transcription with processing. The RNA 5'-capping enzyme associates with the phosphorylated CTD, which facilitates its recruitment to the nascent RNA (Cho et al., 1997; Wada et al., 1998). The CTD associates with 3'-end-processing factors (McCracken et al., 1997; Morris et al., 1999) and truncation of CTD inhibits terminal exon splicing, 3'-end processing, and termination of transcription in vivo (McCracken et al., 1997). RNAP II has been pos-

Reprint requests to: Mariano A. Garcia-Blanco, 424 Carl Building, Box 3053, Duke University Medical Center, Durham, North Carolina 27710, USA; e-mail: garci001@mc.duke.edu.

tulated to be an essential polyadenylation factor (Hirose & Manley, 1998) and the CTD has been implicated in terminal-exon definition and the subsequent 3'-end-processing complex formation (Dye & Proudfoot, 1999). The CTD has also been implicated in coupling RNAP II transcription and splicing; truncation of the CTD leads to a severe impairment of splicing, which correlates with diminished recruitment of splicing factors to sites of transcription (Misteli & Spector, 1999). RNAP II with a hyperphosphorylated CTD (RNAP II<sub>0</sub>) has been shown to stimulate splicing *in vitro*, whereas the non-phosphorylated RNAP II<sub>a</sub> inhibits the reaction (Hirose et al., 1999). This implies that the phosphorylation status of the CTD plays a role in coupling transcription and splicing. As first predicted by Greenleaf (1993), proteins with arginine-serine repeats can interact with the RNAP II<sub>0</sub> CTD (Neugebauer et al., 1995; Yuryev et al., 1996; Du & Warren, 1997; Kim et al., 1997; Tacke & Manley, 1999). Another group of proteins that can potentially link transcription and splicing, the SCAFs (SR-like CTD associated factors), recognize RNAP II<sub>0</sub> phosphorylated at serines 2 and 5 of the heptad repeat (Patturajan et al., 1998).

Previous *in vitro* studies elegantly demonstrated splicing of transcripts generated by RNAP II (Weingartner & Keller, 1981; Kole & Weissman, 1982; Padgett et al., 1983); however, these systems did not splice efficiently and the results were not consistently reproducible (Hernandez & Keller, 1983). Here we report the development of an efficient *in vitro* transcription/splicing system in which the processes occur concurrently. Transcripts generated by RNA polymerase II were accurately and efficiently spliced under reaction conditions that permitted both transcription and splicing to occur simultaneously. In these reactions splicing of RNA-polymerase-II-driven transcripts was accelerated relative to that of transcripts driven by T7 polymerase. Moreover, the product of exon ligation was found associated with the DNA template in reactions driven by RNA polymerase II. These two findings indicate that transcription and splicing were coupled in the *in vitro* system driven by RNA polymerase II. This system should be very useful for the biochemical characterization of interactions between the transcription and splicing machinery.

## RESULTS AND DISCUSSION

### RNAP II transcripts were spliced efficiently and accurately

To obtain robust and simultaneous transcription and splicing *in vitro*, we engineered DNA templates containing the strong HIV-1 long terminal repeat (LTR) RNAP II promoter to drive the synthesis of RNAs with efficient splice sites. These splicing precursors are derived from the first intron of the adenovirus 2 major late transcript. The expected size of the splicing precursor

transcribed from one of these templates, pHA10, was 330 nt and the intron length was 125 nt (Fig. 1A). The buffer conditions were simultaneously optimized for both transcription and splicing (data not shown). The final concentrations of KCl and MgCl<sub>2</sub> were set at 48 mM and 2 mM respectively. The final ATP concentration was 1 mM and the creatine phosphate concentration was kept at 5 mM. Twelve microliters of HeLa cell nuclear extract (14 mg protein/mL) was found to be optimal for the 25- $\mu$ L reaction volume. The same results were obtained using different preparations of HeLa cell nuclear extract (data not shown). Previous reports of cotranscriptional splicing of adenoviral RNA and  $\beta$ -globin RNA used a higher concentration of Mg<sup>+2</sup> (6.0–7.5 mM) with KCl concentrations varying from 0 to 60 mM (Weingartner & Keller, 1981; Kole & Weissman, 1982). Interestingly, later studies on *in vitro* splicing showed a requirement for a lower concentration of Mg<sup>+2</sup> (1.5–2.5 mM) although the concentration of KCl still varied from 28 mM to 50 mM (Hernandez & Keller, 1983; Hardy et al., 1984). The exact conditions used in the experiments shown below are described in detail in Materials and methods.

The pHA10 template was incubated in HeLa nuclear extracts under conditions optimal for simultaneous splicing and transcription. In the reaction shown in Figure 1B, the lariat intermediate, the lariat product, and the product of exon ligation were first clearly detectable at the 30-min time point (Fig. 1B, lanes 3–7). The splicing efficiency for this system appeared to reach a maximum of ~60% after 60 min of incubation (Fig. 1B inset; see the figure legend for the definition of splicing efficiency). As expected, 4  $\mu$ g/mL of  $\alpha$ -amanitin inhibited the synthesis of the splicing precursor and the appearance of splicing intermediates and products; however, other RNA species, including the smear observed in these reactions persisted (data not shown). These data indicate that these RNA species are not degradation products of the splicing precursor, but rather transcripts that were not synthesized by RNAP II. When  $\alpha$ -amanitin was added 40 min after the start of the reaction, the level of splicing precursor and spliced products remained constant for at least another 90 min (data not shown). Using this *in vitro* system, similar efficiencies of splicing were obtained when the adenovirus 2 major late promoter or the cytomegalovirus immediate early promoter were used instead of the HIV-1 LTR to drive the synthesis of the splicing substrates (data not shown). A splicing substrate in which the pHA10 intron was increased in length to nearly 1 kb was also transcribed and spliced efficiently in this system (data not shown). These data indicate that the *in vitro* system described above was capable of efficient splicing of RNAP II driven transcripts.

The fidelity of splice site recognition was analyzed next. The products of RNAP II transcription/splicing reactions and conventional splicing reactions had very

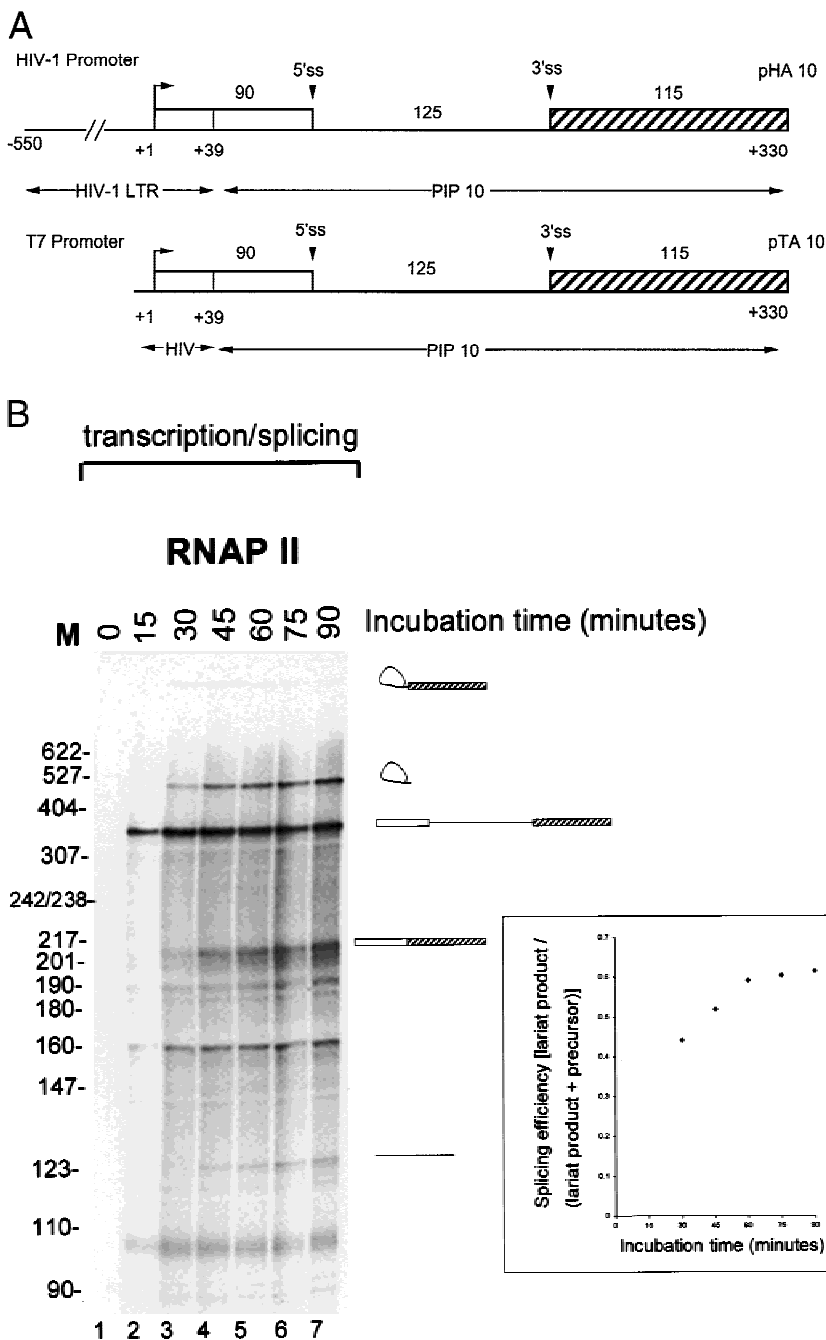


**FIGURE 1.** An in vitro system for efficient splicing of RNAP II transcripts. **A:** Schematic of the DNA templates, pHA10 and pTA10, used for RNAP-II- and T7-RNA-polymerase-driven RNA synthesis, respectively. The RNAP II promoter and the first 39 residues of the 5' exon are from the HIV-1 LTR (−550 to +39) in pHA10. The remainder of the transcription unit is derived from pPIP10 (see Materials and methods). The open and the hatched boxes represent the 5' and 3' exons, respectively. The respective positions of both the 5' and the 3' splice sites are also indicated. pTA10 is identical to pHA10 except that the HIV-1 promoter sequences were replaced with a T7 RNA polymerase promoter. **B:** The RNA products of a RNAP-II-driven transcription-splicing reaction were followed from start to 90 min of incubation in 15 min intervals. Icons to the right of the gel indicate the positions of the different species generated as a result of synthesis and splicing. The icons, from top to bottom, designate the lariat intermediate, lariat product (intron), splicing precursor, the product of exon ligation, and the debranched linear intron. The cleaved 5' exon intermediate was not readily detectable. *Msp*I fragments of pBR322 DNA were used as size markers. Interestingly, the lariat intermediate did not significantly accumulate in the RNAP II system at any time points during the reaction (lanes 3–7), which is quite different from conventional in vitro splicing reactions. Inset: Splicing efficiency was plotted versus time. Splicing efficiency was calculated by the following formula: Splicing efficiency = [moles of lariat product + linear intron (or product of exon ligation)]/[moles of lariat product + linear intron (or product of exon ligation) + moles of splicing precursor]. Very similar values were obtained using the [lariat product + linear intron] or the product of exon ligation.

similar electrophoretic mobility suggesting that the same splice sites were used in both (data not shown). Sequence analysis of cDNAs obtained from the product of exon ligation generated in the RNAP II reactions revealed that splice-site selection and exon ligation occurred at the expected sites (Fig. 2A). When both the terminal guanosines of the intron were mutated to adenosine at the 5' splice site and cytidine at the 3' splice site, respectively, the splicing of the RNAP II transcripts was inhibited (Fig. 2B). All of these results demonstrate that splice site recognition was accurate in the in vitro transcription/splicing system.

### RNAP II transcription enhances the rate of splicing

Quantification of the levels of pHA10 substrate and of its splicing products suggested that splicing was taking place while RNAP II driven transcription was ongoing (Fig. 1B). To more clearly determine the time course of transcript synthesis by RNAP II we used the pHA7-mut template, which encodes a transcript that cannot be spliced (Fig. 2B). There was an apparently linear increase in the level of pHA7-mut transcript up to 60 min of incubation (Fig. 3, left panel), which was consistent

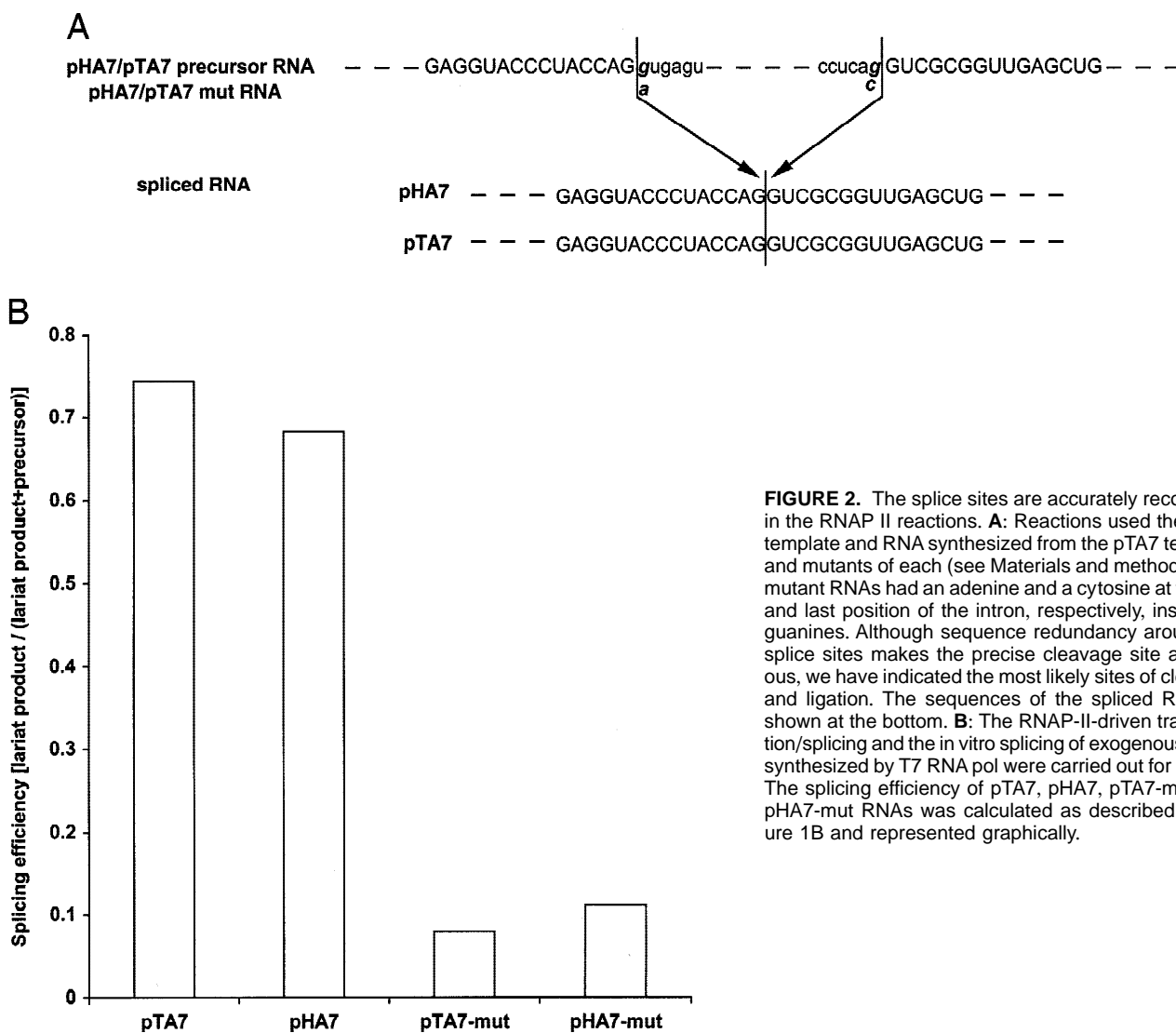


**FIGURE 2.** The splice sites are accurately recognized in the RNAP II reactions. **A:** Reactions used the pHA7 template and RNA synthesized from the pTA7 template and mutants of each (see Materials and methods). The mutant RNAs had an adenine and a cytosine at the first and last position of the intron, respectively, instead of guanines. Although sequence redundancy around the splice sites makes the precise cleavage site ambiguous, we have indicated the most likely sites of cleavage and ligation. The sequences of the spliced RNA are shown at the bottom. **B:** The RNAP-II-driven transcription/splicing and the *in vitro* splicing of exogenous RNAs synthesized by T7 RNA pol were carried out for 90 min. The splicing efficiency of pTA7, pHA7, pTA7-mut, and pHA7-mut RNAs was calculated as described in Figure 1B and represented graphically.

with calculations based on reactions using pHA10. A parallel reaction using pTA7-mut and T7 RNA polymerase added to the HeLa nuclear extract (to a final reaction concentration of 0.4 U/ $\mu$ L) revealed that transcription of the pTA7-mut RNA also appeared to be linear for the first 60 min of incubation (Fig. 3, right panel). The absolute levels of pTA7-mut transcripts depended on the concentration of T7 RNA polymerase added to the nuclear extract (data not shown). The time course of splicing for pHA10 RNA and the time course for transcription of the mutant transcripts, taken together, suggest that the splicing of pHA10 RNAs was concurrent with active transcription (compare Fig. 1B, inset, with Fig. 3, left panel).

If transcription and splicing were coupled in the RNAP II *in vitro* system, one would expect that the transcriptional machinery would affect the splicing reaction, presumably enhancing the rate of splicing. When comparing the rates of splicing between the RNAP II system and conventional splicing reactions, we did not notice re-

markable enhancement of splicing kinetics (data not shown; see legend to Fig. 1B). The conventional splicing reactions, however, commence with a large excess of splicing substrate, whereas the RNAP II system requires the synthesis of this substrate. Supplementing the HeLa nuclear extract with T7 RNA polymerase and carrying out simultaneous synthesis and splicing would provide a much more valid comparison for RNAP II transcription/splicing reactions. This gives the splicing machinery the same opportunity to act on nascent substrates synthesized by the two different polymerases. pHA10 and pTA10 templates were incubated at 30°C for identical periods of time and their RNA products, which are encoded by identical sequences in the two templates (see Fig. 1A and discussion below), were analyzed as discussed before. Interestingly, we observed a significantly faster accumulation of splicing products in the RNAP II reactions relative to the T7 RNA polymerase reactions (Fig. 4A). Lariat intermediates were detected at 30 min of incubation and lariat

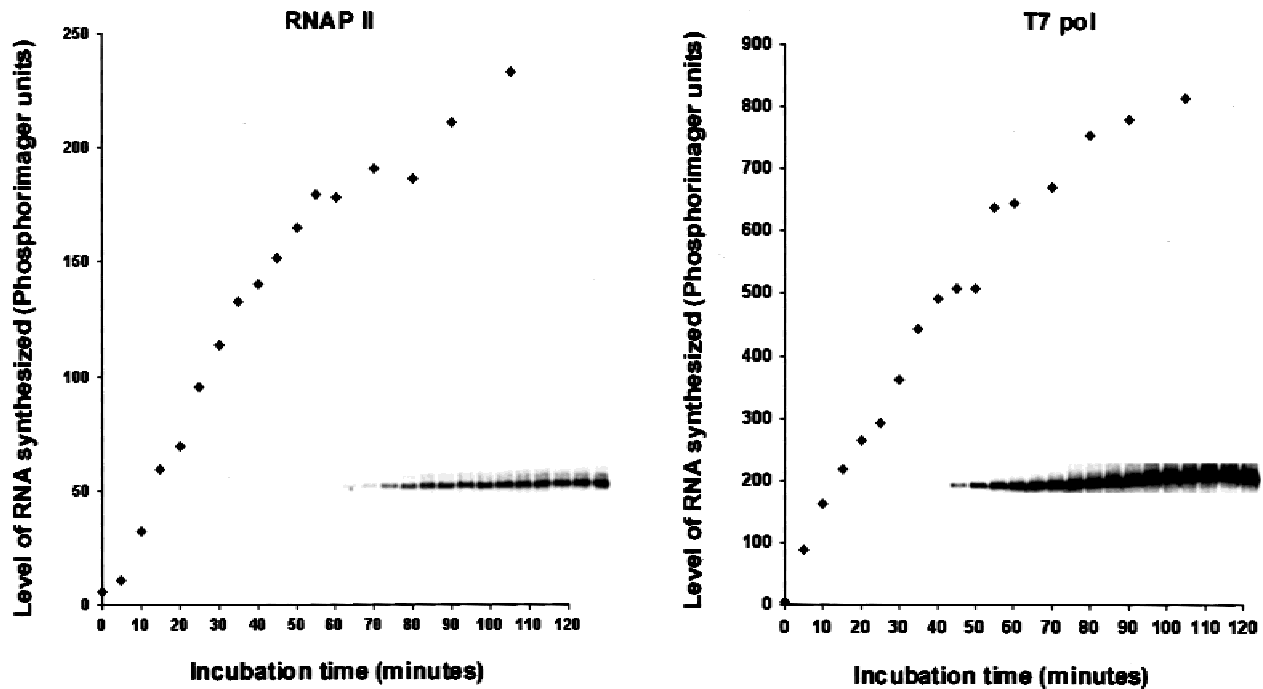


**FIGURE 3.** RNA synthesis by RNAP II and splicing are occurring concurrently in the transcription/splicing system. Quantification of RNA synthesis in the RNAP II and T7 pol reactions are plotted *versus* time. pHA7-mut and pTA7-mut templates were used for transcription and the aliquots were taken out at 5-min intervals. The amount of RNA in each band was calculated as total counts (in phosphorimager units) divided by the number of uridines present in them. Minimal degradation was assumed based on the data described in the text.

products at 40 min in RNAP II reactions, whereas these were not detectable in T7 pol reactions until 50 min (Fig. 4A). Even though the absolute kinetics of the reactions varied slightly between experiments, the significant enhancement of splicing in RNAP II reactions was always observed. Splicing was calculated using the formula described in the legend to Figure 1. Calculations using the product of exon ligation were sometimes made difficult by the appearance of a nonspecific transcript in some T7 RNA polymerase reactions (see, for example, Fig. 4A, lanes 9 and 10). This species, which migrated immediately above the product of exon ligation, was observed in reactions that do not have any lariat or linear intron product. To circumvent this problem and to confirm our results with a different assay, we measured splicing using a RT-PCR assay that was shown to be quantitative for the range of transcript concentrations used. Transcripts generated by RNAP II were spliced faster than the T7-polymerase-generated RNAs even though the level of precursor in the latter was at least equal or higher in all the time points studied. In the RNAP II reactions the product of exon ligation was first detected at 45 min of incubation and its level gradually increased with time (Fig. 4B). For T7-RNA-pol-derived transcripts, spliced product was not detected until 60 min after the start of the reaction (Fig. 4B). Thus the RT-PCR assay corroborated the results obtained using the direct labeling of transcripts. These data indicate that the synthesis of splicing sub-

strates by RNAP II enhances the rate of splicing and imply that this *in vitro* system recapitulates the functional coupling that has been suggested by *in vivo* experiments.

RNAP II transcription can lead to transcript modification and these modifications could explain the splicing rate enhancement. The most likely modification that may account for splicing differences is 5' capping, which in some *in vitro* splicing systems has been shown to be critical for efficient splicing (Konarska et al., 1984). In our system, splicing of pTA10 was unaffected by capping (Fig. 5A). To rule out other modifications between the RNAs, splicing substrates synthesized by RNAP II and by T7 RNA polymerase were purified and incubated further under the splicing conditions described above. The rates of splicing of the two transcripts were indistinguishable (Fig. 5B). These experiments suggest that intrinsic differences in the structure of the splicing substrates do not determine the enhancement in splicing seen in the RNAP II reactions. The addition of the 5' cap may be a critical determinant of splicing efficiency, however, in other systems where capping has been shown to be critical for *in vitro* splicing (Izaurralde et al., 1994). Nonetheless, our data suggest that the functional coupling observed between RNAP II transcription and splicing could be mediated by interactions other than those involving the 5' cap. At this time there are no *in vivo* data that directly address this issue.

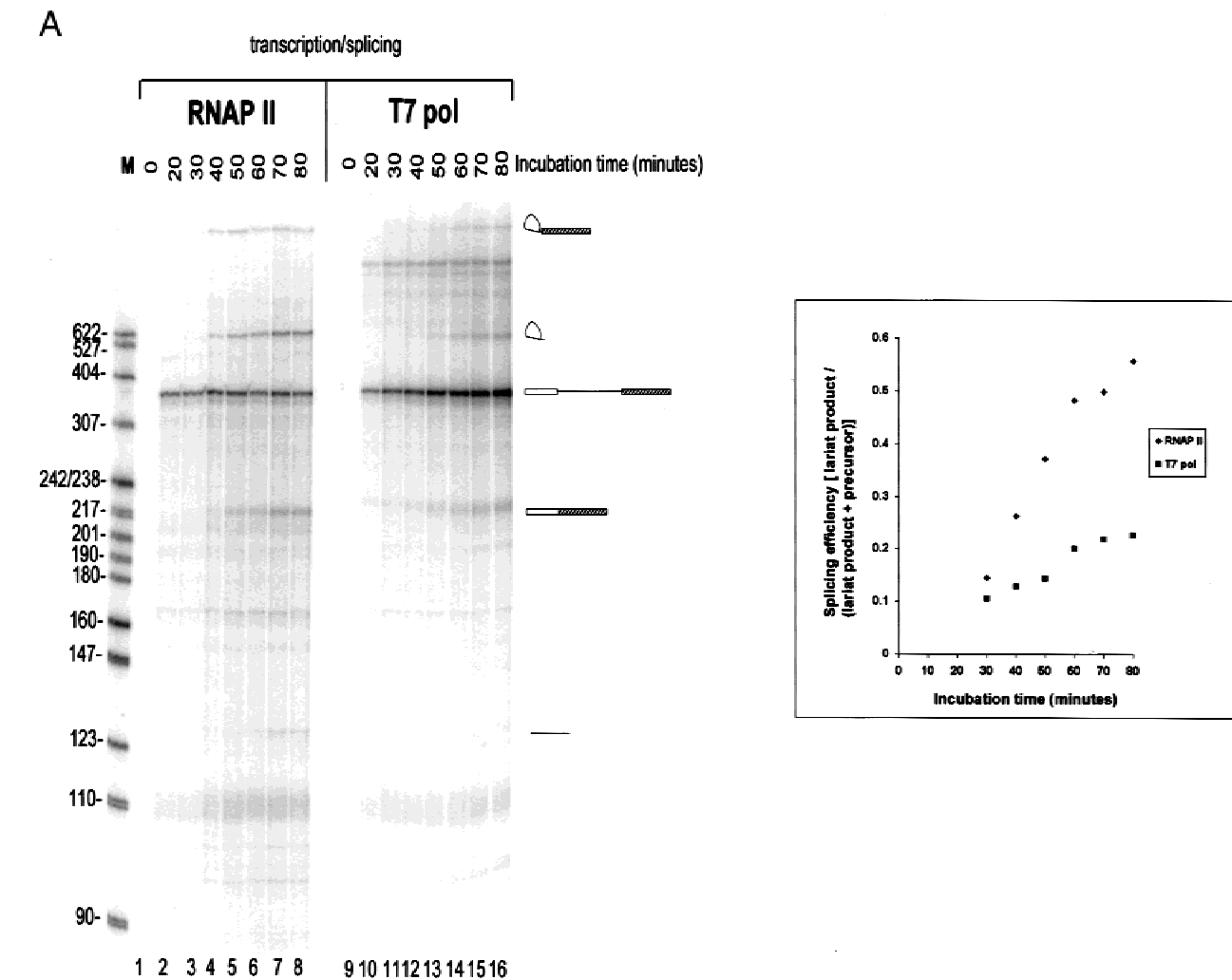
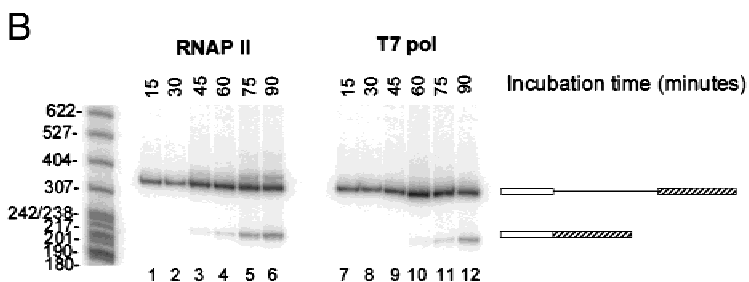


**FIGURE 4.** RNAP II transcription enhances the rate of splicing. **A:** Both the pHA10 (lanes 1–8) and pTA10 (lanes 9–16) templates were used to synthesize the splicing precursors under identical conditions. T7 RNA polymerase (0.4 U/ $\mu$ L) were used to drive transcription from pTA10 templates. The reactions were incubated at 30 °C from 0 to 80 min ( $t = 0$ , lanes 1 and 9;  $t = 20$ , lanes 2 and 10;  $t = 30$ , lanes 3 and 11;  $t = 40$ , lanes 4 and 12;  $t = 50$ , lanes 5 and 13;  $t = 60$ , lanes 6 and 14;  $t = 70$ , lanes 7 and 15;  $t = 80$ , lanes 8 and 16). *Msp*I fragments of pBR322 DNA were used as size markers. For description of the icons, see legend to figure 1A. Inset: Splicing efficiency for both the reactions were plotted *versus* time. (See legend to Fig. 1B for description). **B:** RT-PCR quantification of spliced products. RNA extracted after the designated time periods was amplified with exon-specific primers (See Materials and methods). Aliquots of the reaction were assayed at 15-min intervals ( $t = 15$ , lanes 1 and 7;  $t = 30$ , lanes 2 and 8;  $t = 45$ , lanes 3 and 9;  $t = 60$ , lanes 4 and 10;  $t = 75$ , lanes 5 and 11;  $t = 90$ , lanes 6 and 12). *Msp*I fragments of pBR322 DNA were used as size markers. The PCR product corresponding to the splicing precursor (top icon) was 330 bp and that corresponding to the spliced product was 205 bp (bottom icon).



### Splicing of nascent RNAP II transcripts *in vitro*

Above we have shown that the RNAP II transcripts were spliced while transcription is ongoing and that the

transcripts generated by RNAP II were spliced faster than those synthesized by T7 RNA polymerase. It was not clear, however, whether or not splicing occurred on nascent transcripts still tethered to RNAP II. Biotinyl-

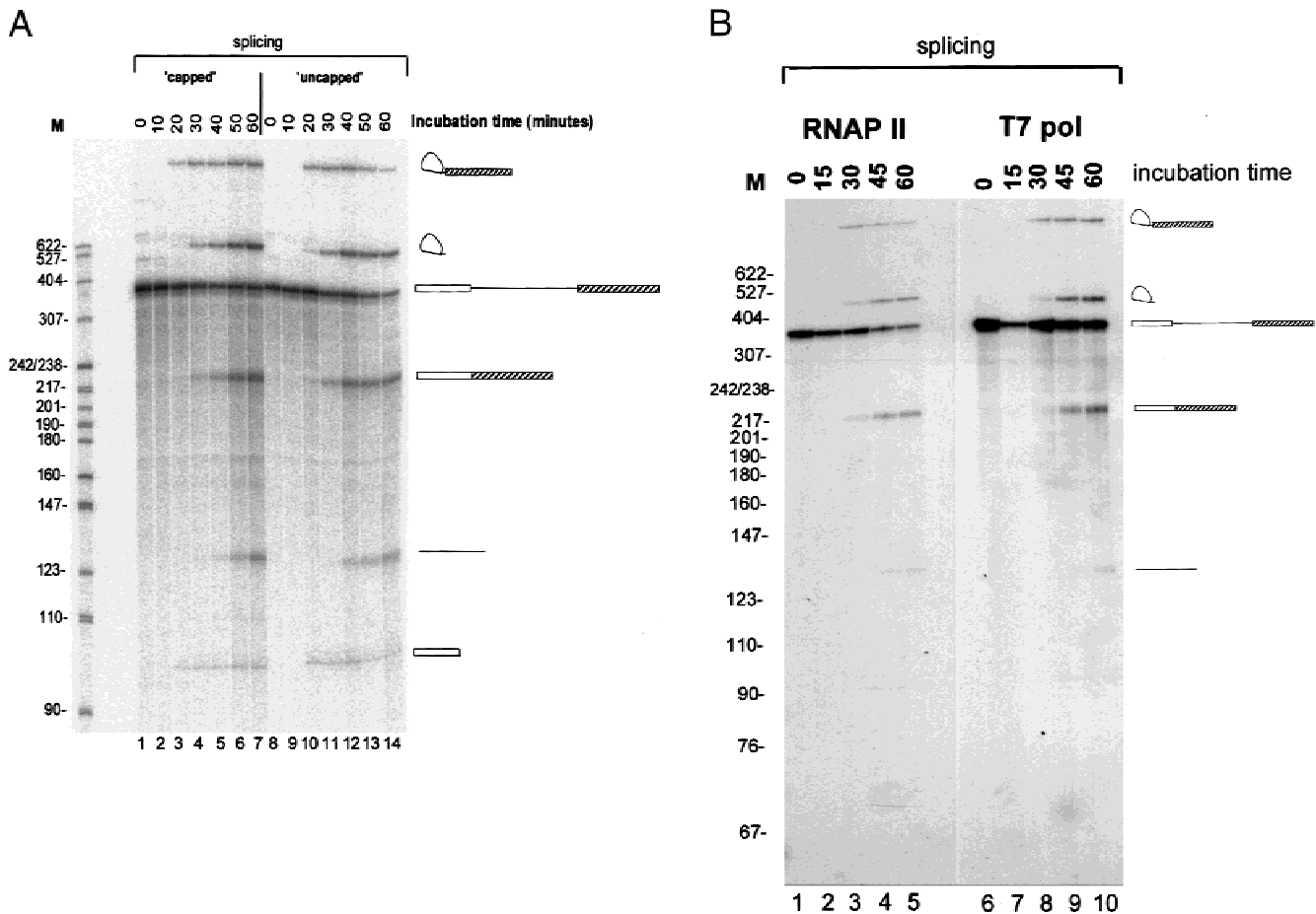


**FIGURE 5.** The RNA products of RNAP II and T7 RNA polymerase are spliced with similar kinetics. **A:** pTA10 was used to make capped and uncapped versions of pTA10 RNAs, which were purified and incubated under splicing conditions (see Materials and methods). The capped and uncapped versions of pTA10 spliced with very similar kinetics under the reaction conditions described in the text. Icons to the right of the gel indicate the positions of the different species generated as a result of splicing (for description of these icons, see legend to Fig. 1B). In these reactions the cleaved 5' exon intermediate was detectable and is identified with the last icon near the bottom. **B:** Splicing substrates synthesized with either RNAP II or T7 pol were purified and incubated in splicing reactions *in vitro*. Reactions were terminated at 15-min intervals from time 0 to 60 min of incubation and the products of the reaction evaluated. Icons to the right of the gel indicate the positions of the different species generated as a result of splicing (for description of these icons, see legend to Fig. 1B).

ated transcription templates pHA10, pHA7-mut, and pTA10 were incubated in HeLa nuclear extracts as described above (see Materials and methods). To test whether spliced products were associated with the templates, these were bound to streptavidin beads and separated magnetically. As expected, a fraction of the pHA10 splicing precursor was found associated with the pHA10 template in reactions incubated for 15 min or 45 min (Fig. 6, lanes 1–6). The product of exon ligation was found associated with the pHA10 template at 45 min of incubation (Fig. 6, lanes 4–6). The amount of both precursor and the spliced product obtained after RT-PCR was quantified using a phosphorimager and the ratio of spliced product to precursor RNA was calculated in all the cases. The ratio obtained in the bound pHA10 template after 45 min of reaction closely matched that observed in the supernatant fraction, suggesting that the bulk of the splicing at 45 min was taking place among template-bound transcripts. Not sur-

prisingly, the pHA7-mut did not lead to the production of exon-ligated product (Fig. 6, lanes 7–12). pTA10 was incubated identically, except that the HeLa nuclear extract was supplemented with T7 RNA polymerase. Interestingly, the pTA10 product of exon ligation was not found associated with the template, even though a sizeable fraction of the splicing substrate was (Fig. 6, lanes 13–18). Finding RNAP-II-driven spliced products associated with templates implies that splicing was occurring while the transcript was still engaged by the polymerase. This demonstrates physical coupling between the transcription and splicing machinery.

#### Coupling of RNAP II transcription and splicing *in vitro*

It was shown *in vivo* that RNAP II, while elongating nascent RNAs, also stimulates their subsequent processing (Corden & Patturajan, 1997; Du & Warren, 1997;

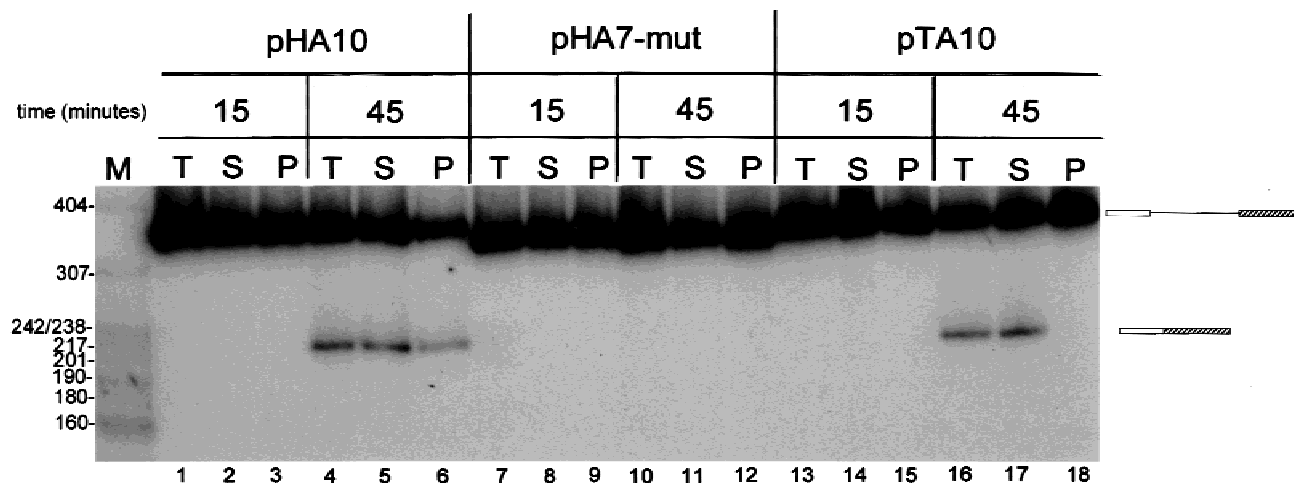


**FIGURE 6.** Splicing of nascent RNAP II transcripts in vitro. The RT-PCR analysis of the RNA molecules attached to the DNA templates is shown. The biotinylated pHA10 (lanes 1–6), pHA7-mut (lanes 7–12), and pTA10 (lanes 13–18) templates were pulled down with streptavidin-magnetic particles after 15 and 45 min at 30 °C and bound RNA molecules were analyzed by RT-PCR. For transcription from the pTA10 template, T7 RNA polymerase (0.8 U/ $\mu$ L) was added per reaction. The total (T) reaction content, the supernatant fraction (S) after magnetic separation, and the pellet fraction (P) for each template were analyzed. The identities of the RNA species recovered are indicated to the right. The PCR product corresponding to the pHA10 splicing precursor (top icon) was 330 bp and that corresponding to the spliced product was 205 bp (bottom icon). The PCR product corresponding to pHA7-mut was 310 bp. *MspI* fragments of pBR322 DNA were used as size markers.

Steinmetz, 1997; Bentley, 1999). The present study demonstrates a highly efficient in vitro system for the coupled transcription and splicing of nascent RNAP II transcripts. Functional coupling was shown by a rate enhancement in RNAP II reactions. Quantification of this enhancement suggests that it is spliceosome assembly that is accelerated, leading to a reduction in the lag phase of splicing. It is likely that RNAP II promotes the formation of splicing complexes on nascent transcripts, but would not necessarily affect the rate of the chemical steps in splicing. This is consistent with studies demonstrating that RNAP II stimulates the early steps of spliceosome assembly in a system where splicing was otherwise crippled (Hirose et al., 1999). As has been proposed in vivo, RNAP II transcripts were spliced as nascent RNAs in the in vitro system described here. This system can be employed to address questions regarding the physical associations between components of the transcription and splicing machinery and will be useful in elucidating the molecular underpinnings of in vivo phenomena linking RNAPII and processing of pre-mRNAs. The present study can also help in understanding the effects of promoter elements on RNA alternative splicing and role of different splicing factors in connecting these important cellular processes.

## MATERIALS AND METHODS

### Template DNA

A fragment derived from the HIV-LTR (–550 to +39) was excised from pBC/HIV/SEAP (Bohjanen et al., 1997) by *StyI*/

*SacI* digestion and inserted immediately upstream of the *EcoRI*/*HindIII* fragment of PIP10 (Carstens et al., 1998) and the entire construct was cloned in pBluescript SK(–) (Stratagene) to generate the plasmid pHA10. The SK primer (Stratagene) and a primer directed against the HIV-LTR (5'-CTCTAGGCTCCAAAAAAGCCTCC-3') were used to generate RNAP II transcription templates; for T7 RNA pol transcription, the pTA10 template was generated using SK-primer and a chimeric primer having T7 RNA pol promoter sequences around the transcription initiation of the HIV-1 LTR (5'-TCCCCCGGGTAATACGACTCACTATA GGGTCTCTCTGGTTAGACCA-3'). pHA7 and pHA7-mut and pTA7 and pTA7-mut templates contained the identical HIV-1 or T7 promoter sequences linked to the *EcoRI*/*HindIII* fragment of PIP7 or PIP7 with the first and last intronic residue mutated (see text and the legend to Fig. 2) (Pasman & Garcia-Blanco, 1996).

### In vitro transcription and splicing

Nuclear extracts were prepared by the method of Dignam et al. (1983). The in vitro transcription and splicing reactions were carried out at 30 °C for the indicated times in 25  $\mu$ L of a mix containing 12  $\mu$ L HeLa nuclear extract (14 mg protein/mL), 9.6 mM HEPES-KOH, pH 7.9, 9.6% (v/v) glycerol, 48 mM KCl, 2 mM MgCl<sub>2</sub>, 300 ng poly(dI):poly(dC) (Amersham Pharmacia Biotech), 250 ng poly I:poly C (Amersham Pharmacia Biotech), 240  $\mu$ M DTT, 5 mM creatine phosphate, 120  $\mu$ M EDTA, 1 U of RNasin (Promega), 600  $\mu$ M of GTP and CTP, 1 mM ATP, 40  $\mu$ M UTP, and 10  $\mu$ Ci of [ $\alpha$ -<sup>32</sup>P]UTP (3,000 Ci/mmol) (NEN). The template DNA was used at 100 ng per reaction mixture for the RNAP II system. For cotranscriptional splicing of the nascent T7-RNA-polymerase-generated transcripts, the template DNA (pTA10) contained T7 promoter instead of the HIV-LTR. The reactions were performed under



identical conditions with 50 ng of template DNA and 10 units of T7 RNA polymerase (Ambion) per 25  $\mu$ L reaction. For *in vitro* splicing, 50 fmol of T7-RNA-polymerase-generated splicing substrate was added exogenously. The RNA transcripts for *in vitro* splicing were synthesized to the same specific activity as RNAs generated by RNAP II and were capped using a fourfold molar excess of cap analog (New England Biolabs) over GTP during their synthesis (Konarska et al., 1984). To terminate the reaction for both transcription/splicing and *in vitro* splicing, 100  $\mu$ L of 100 mM Tris-HCl, pH 7.5, 200 mM NaCl, 100 mM EDTA, 300 mM NaOAc, 25  $\mu$ g of yeast tRNA per mL, 0.75% sodium dodecyl sulfate (SDS), 50  $\mu$ L of 10 mM Tris-HCl, pH 7.5, 50 mM EDTA, 7 M urea, 0.1 M LiCl, and 0.5% SDS (w/v) were added. RNA was deproteinized once with phenol:chloroform:isoamyl alcohol (25:24:1) and once with chloroform:isoamyl alcohol (24:1). The extracted RNA was precipitated with 50  $\mu$ L of 7.5 M ammonium acetate and 600  $\mu$ L of chilled ethanol and resuspended in H<sub>2</sub>O. For debranching reactions with HeLa S100 fraction, RNA was treated with 15  $\mu$ L of HeLa S100 fraction (Dignam et al., 1983) in a 25- $\mu$ L reaction volume containing 8 mM EDTA at 30 °C for 10 min. The RNA was deproteinized and precipitated as before. For analysis of the reaction products, pellets were resuspended in 98% formamide buffer and resolved by electrophoresis in 12% polyacrylamide-8 M urea gels. The activity of specific bands was quantified using a PhosphorImager (Molecular Dynamics) and the amount of each RNA species was determined based on their uridine content.

### Pull-down and RT-PCR analysis

The biotinylated DNA templates used for pull-down assays were generated by PCR with the biotinylated primers specific for the promoter sequences. After the transcription/splicing reactions were incubated for the desired period, the DNA molecules were separated magnetically with 10  $\mu$ L streptavidin magnetic particles (Boehringer Mannheim) and washed at least three times with 100  $\mu$ L TEN-100 (10 mM Tris-HCl, pH 7.5, 1 mM EDTA, and 100 mM NaCl), and particle-bound nucleic acids were phenol:chloroform extracted and precipitated with ethanol as discussed above. The precipitates were resuspended in 1 $\times$  RQ1 DNase buffer (40 mM Tris-HCl, pH 8.0, 10 mM MgSO<sub>4</sub>, and 1 mM CaCl<sub>2</sub>) and treated with 1 U RQ1 DNase I (Promega) for 30 min at 37 °C. The reaction was stopped by incubating at 65 °C for 10 min with 2 mM EGTA. Five microliters from this sample were reverse transcribed with 200 U of MMLV-RT (Gibco BRL) and then PCR amplified for 40 cycles with 2.5 U of Taq DNA polymerase (Gibco BRL) using primers specific for the ends of the exons. For quantitative RT-PCR, the amount of MMLV-RT was reduced to 100 U per reaction and 0.1 U of Taq DNA polymerase (Gibco BRL) were added for PCR amplification for 20 cycles. The PCR products were separated in a nondenaturing 8% polyacrylamide gel.

### ACKNOWLEDGMENTS

We thank members of the Garcia-Blanco and Keene laboratories for many useful discussions and suggestions. In particular we thank Russ Carstens and Aaron Goldstrohm for

critical reading of the manuscript and Annette Kennett for help in its preparation. This work was funded by grants from the American Cancer Society and an Established Investigator Award from the American Heart Association to M.A.G.B.

Received December 7, 1999; returned for revision January 12, 2000; revised manuscript received May 6, 2000

### REFERENCES

- Bauren G, Wieslander L. 1994. Splicing of Balbani ring 1 gene pre-mRNA occurs simultaneously with transcription. *Cell* 76:183–192.
- Bentley D. 1999. Coupling RNA polymerase II transcription with pre-mRNA processing. *Curr Opin Cell Biol* 11:347–351.
- Beyer AL, Osheim YN. 1988. Splice site selection, rate of splicing, and alternative splicing of nascent transcripts. *Genes & Dev* 2:754–765.
- Bohjanen PR, Liu Y, Garcia-Blanco MA. 1997. TAR RNA decoys inhibit tat-activated HIV-1 transcription after preinitiation complex formation. *Nucleic Acids Res* 25:4481–4486.
- Carstens RP, McKeehan WL, Garcia-Blanco MA. 1998. An intronic sequence element mediates both activation and repression of rat fibroblast growth factor receptor 2 pre-mRNA splicing. *Mol Cell Biol* 18:2205–2217.
- Cho EJ, Takagi T, Moore CR, Buratowski S. 1997. mRNA capping enzyme is recruited to the transcription complex by phosphorylation of the RNA polymerase II carboxy-terminal domain. *Genes & Dev* 11:3319–3326.
- Corden JL, Patturajan M. 1997. A CTD function linking transcription to splicing. *Trends Biochem Sci* 22:413–416.
- Cramer P, Caceres JF, Cazalla D, Kadener S, Muro AF, Baralle FE, Kornblihtt AR. 1999. Coupling of transcription with alternative splicing: RNA pol II promoters modulate SF2/ASF and 9G8 effects on an exonic splicing enhancer. *Mol Cell* 4:251–258.
- Cramer P, Pesce CG, Baralle FE, Kornblihtt AR. 1997. Functional association between promoter structure and transcript alternative splicing. *Proc Natl Acad Sci USA* 94:11456–11460.
- Dignam JD, Lebovitz RM, Roeder RG. 1983. Accurate transcription initiation by RNA polymerase II in a soluble extract from isolated mammalian nuclei. *Nucleic Acids Res* 11:1475–1489.
- Du L, Warren SL. 1997. A functional interaction between the carboxy-terminal domain of RNA polymerase II and pre-mRNA splicing. *J Cell Biol* 136:5–18.
- Dye MJ, Proudfoot NJ. 1999. Terminal exon definition occurs cotranscriptionally and promotes termination of RNA polymerase II. *Mol Cell* 3:371–378.
- Greenleaf AL. 1993. Positive patches and negative noodles: Linking RNA processing to transcription? *Trends Biochem Sci* 18:117–119.
- Hardy SF, Grabowski PJ, Padgett RA, Sharp PA. 1984. Cofactor requirements of splicing of purified messenger RNA precursors. *Nature* 308:375–377.
- Hernandez N, Keller W. 1983. Splicing of *in vitro* synthesized messenger RNA precursors in HeLa cell extracts. *Cell* 35:89–99.
- Hirose Y, Manley JL. 1998. RNA polymerase II is an essential mRNA polyadenylation factor. *Nature* 395:93–96.
- Hirose Y, Tacke R, Manley JL. 1999. Phosphorylated RNA polymerase II stimulates pre-mRNA splicing. *Genes & Dev* 13:1234–1239.
- Izaurralde E, Lewis J, McGuigan C, Jankowska M, Darzynkiewicz E, Mattaj JW. 1994. A nuclear cap binding protein complex involved in pre-mRNA splicing. *Cell* 78:657–668.
- Jimenez-Garcia LF, Spector DL. 1993. *In vivo* evidence that transcription and splicing are coordinated by a recruiting mechanism. *Cell* 73:47–59.
- Kim E, Du L, Bregman DB, Warren SL. 1997. Splicing factors associate with hyperphosphorylated RNA polymerase II in the absence of pre-mRNA. *J Cell Biol* 136:19–28.
- Kole R, Weissman SM. 1982. Accurate *in vitro* splicing of  $\beta$ -globin RNA. *Nucleic Acids Res* 10:5429–5445.
- Konarska MM, Padgett RA, Sharp PA. 1984. Recognition of cap structure in splicing *in vitro* of mRNA precursors. *Cell* 38:731–736.

- McCracken S, Fong N, Yankulov K, Ballantyne S, Pan G, Greenblatt J, Patterson SD, Wickens M, Bentley DL. 1997. The C-terminal domain of RNA polymerase II couples mRNA processing to transcription. *Nature* 385:357–361.
- Misteli T, Spector DL. 1999. RNA polymerase II targets pre-mRNA splicing factors to transcription sites in vivo. *Mol Cell* 3:697–705.
- Morris DP, Phatnani HP, Greenleaf AL. 1999. Phospho-carboxyl-terminal domain binding and the role of a prolyl isomerase in pre-mRNA 3'-end formation. *J Biol Chem* 274:31583–31587.
- Neugebauer KM, Roth MB. 1997. Transcription units as RNA processing units. *Genes & Dev* 11:3279–3285.
- Neugebauer KM, Stolk JA, Roth MB. 1995. A conserved epitope on a subset of SR proteins defines a larger family of pre-mRNA splicing factors. *J Cell Biol* 129:899–908.
- Padgett RA, Hardy SF, Sharp PA. 1983. Splicing of adenovirus RNA in a cell-free transcription system. *Proc Natl Acad Sci USA* 80:5230–5234.
- Pasman Z, Garcia-Blanco MA. 1996. The 5' and 3' splice sites come together via a three dimensional diffusion mechanism. *Nucleic Acids Res* 24:1638–1645.
- Patturajan M, Wei X, Berezney R, Corden JL. 1998. A nuclear matrix protein interacts with the phosphorylated C-terminal domain of RNA polymerase II. *Mol Cell Biol* 18:2406–2415.
- Roberts GC, Gooding C, Mak HY, Proudfoot NJ, Smith CW. 1998. Co-transcriptional commitment to alternative splice site selection. *Nucleic Acids Res* 26:5568–5572.
- Steinmetz EJ. 1997. Pre-mRNA processing and the CTD of RNA polymerase II: The tail that wags the dog? *Cell* 89:491–494.
- Tacke R, Manley JL. 1999. Functions of SR and Tra2 proteins in pre-mRNA splicing regulation. *Proc Soc Exp Biol Med* 220:59–63.
- Wada T, Takagi T, Yamaguchi Y, Ferdous A, Imai T, Hirose S, Sugimoto S, Yano K, Hartzog GA, Winston F, Buratowski S, Handa H. 1998. DSIF, a novel transcription elongation factor that regulates RNA polymerase II processivity, is composed of human Spt4 and Spt5 homologs. *Genes & Dev* 12:343–356.
- Weingartner B, Keller W. 1981. Transcription and processing of adenoviral RNA by extracts from HeLa cells. *Proc Natl Acad Sci USA* 78:4092–4096.
- Yuryev A, Patturajan M, Litingtung Y, Joshi RV, Gentile C, Gebara M, Corden JL. 1996. The C-terminal domain of the largest subunit of RNA polymerase II interacts with a novel set of serine/arginine-rich proteins. *Proc Natl Acad Sci USA* 93:6975–6980.
- Zhang G, Taneja KL, Singer RH, Green MR. 1994. Localization of pre-mRNA splicing in mammalian nuclei. *Nature* 372:809–812.